EURO LETTERS nanotox Vol. 3 (2011), 001, 0001-0011
journal homepage: http://www.euro-nanotox-letters.com

Transport of metal oxide nanoparticles across Calu-3 cell monolayers modelling the air-blood barrier

Christine Schulze[a], Ulrich F. Schaefer[a], Matthias Voetz[b], Wendel Wohlleben[c], Cornel Venzago[d], Claus-Michael Lehr[a,e*]

[a] *Department of Biopharmaceutics and Pharmaceutical Technology, Saarland University, Saarbruecken, Germany*

[b] *PT-MT-Materials Characterization & Testing, Bayer Technology Services GmbH, Leverkusen, Germany*

[c] *Polymer Physics Research, BASF SE, Ludwigshafen, Germany*

[d] *AQura GmbH, Hanau-Wolfgang, Germany*

[e] *Department of Drug Delivery (DDEL), Helmholtz-Institute for Pharmaceutical Research (HIPS), Helmholtz Center for Infection Research (HZI), Saarland University, Saarbruecken, Germany*

ARTICLE INFO: Research Article

Article History:
Received: 18.02.2011
Pre-Published: 28.02.2011
Accepted: 14.06.2011
Available online: 14.07.2011

Keywords:
Particle transport, TEER, *in vitro* model, permeability, lung, inhalation toxicology

DOI number:
10.1515/entl-2015-0003

ABSTRACT

As inhalation is the major exposure route for nanoparticles, the question if inhaled particles can overcome the respiratory epithelial barrier and hence enter the body is of great interest. Here, we adapted the for soluble substances well established Calu-3 *in vitro* air-blood barrier model to the use of nanoparticle transport testing. As the usually used filter supports hindered particle transport due to their small pore size, supports with a pore size of 3 µm had to be used. On those filters, barrier and transport characteristics of the cells were tested and culture conditions changed to obtain optimal conditions. Functionality was confirmed with transport experiments with polystyrene model particles prior to testing of industrially relevant engineered metal oxide particles. Except for CeO_2 nanoparticles, no transport across the epithelial barrier model could be detected. Paracellular permeability and barrier function was not affected by any of the nanoparticles, except for ZrO_2.

INTRODUCTION

Inhalation of nanoparticles into the lung is probably the most important route for nanoparticle exposure, especially as translocation of nanoparticles over the air-blood barrier into secondary target organs was recently proven in rats for iridium and carbon nanoparticles (Kreyling et al., 2009). Translocation across the respiratory epithelium to access the blood stream might bear some risks, as numerous publications report cytotoxic effects or the provocation of oxidative stress in *in vitro* assays for silver (AshaRani et al., 2009; Carlson et al., 2008), iron oxide and manganese oxide (Choi et al., 2009) and silica nanoparticles (Wahl et al., 2008). Hence, the safety of nanoparticles is a major issue that needs attention and further investigation. Some *in vivo* inhalation and instillation experiments have been performed, mostly in rats, already. But for broad testing, *in vitro* assays were simpler, less time consuming, cheaper and ethically unproblematic.

***Corresponding author: Claus-Michael Lehr,** Biopharmaceutics and Pharmaceutical technology, Saarland University, Campus, building A4.1, Saarbruecken, Germany and Department of Drug Delivery (DDEL), Helmholtz-Institute for Pharmaceutical Research (HIPS), Helmholtz Center for Infection Research (HZI), Saarland University, Saarbruecken, Germany
e-mail:lehr@mx.uni-saarland.de

ISSN: 2074-8515/€ - see front matter, EURO-NanoTox 2011

Grown on so called Transwell® filter devices, Calu-3 cells develop a tight monolayer, mimicking the respiratory epithelium. In contrast to other *in vitro* lung models like the cell line A549, they develop tight junctions, which are the prerequisite for cell polarity and the resulting barrier function. (Forbes and Ehrhardt, 2005). This model is well-known and characterized for soluble substances, e.g. pharmaceutically relevant chemicals, already (Florea et al., 2003; Forbes and Ehrhardt, 2005; Lehr et al., 2006; Mathias et al., 1996; Sakagami, 2006; Sporty et al., 2008). As phagocytic as well as endocytic pathways of entry into the cell are described for nanoparticles (Hillaireau and Couvreur, 2009), transcellular transport could be a relevant route for particle translocation across the respiratory epithelium.

However, some adaptations might be required for transport experiments with nanoparticles, as the pore size of the usually used filter inserts with a pore diameter of 0.4 µm might be a significant barrier for the nanoparticle transport. Still, replacing those filters with inserts with a larger pore size of 3 µm might bring up difficulties in cell culturing, as those filter inserts reveal different properties (see Figure 1). As demonstrated for A549 cells already (Rothen-Rutishauser et al., 2005), the cells could grow into the pores or even on both sides of the filters, clogging the pores and hence negating particle transport. Also, the cells could alter their morphology or lose their barrier function. In this publication, those subjects were addressed to optimize the Calu-3 transport model for particle transport experiments. To test functionality of the adapted model, transport experiments with polystyrene model particles were performed prior of using this model for transport experiments with commercially available ZrO_2, AlOOH and two different TiO_2 and CeO_2 nanoparticles.

pore size	**0.4 µm**	**3 µm**
	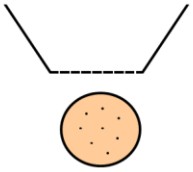	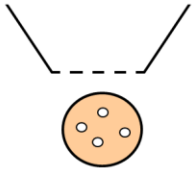
radius	0.00002 cm	0,00015 cm
number of pores	$4*10^6$	$2*10^6$
total filter area	1.12 cm^2	1.12 cm^2
area of one pore	$1.25*10^{-9}$ cm^2	$7*10^{-8}$ cm^2
area of all pores (= diffusion area)	0.005 cm^2	0.14 cm^2
relation pore area 3 µm/0.4 µm	28	
problems	NP may not pass filter due to their size (0.05-0.2 µm)	Cells may grow through the pores or on both sides of the filter

Figure 1*: Comparison of Transwell® filter systems for use in transport assays: For transport studies with dissolved drugs, a pore size of 0.4 µm is sufficient, but for nanoparticle transport, an adaptation to a larger pore size of 3 µm might be necessary. All specifications are made for one filter insert.*

MATERIALS AND METHODS

MATERIALS. Polystyrene nanoparticles were purchased from Polysciences Europe GmbH, Eppelheim, Germany. All ingredients for Krebs-Ringer buffer (KRB; 114.2 mM NaCl, 3 mM KCl, 1.5 mM K_2HPO_4 x 3 H_2O, 10 mM HEPES, 4 mM D-Glucose, 1.4 mM $CaCl_2$, 2.56 mM $MgCl_2$) and PBS (137 mM NaCl, 8.1 mM Na_2HPO_4 x H_2O, 2.7 mM KCl, 1.5 mM KH_2PO_4, pH 7.4), as well as bovine serum albumin, Na-fluorescein, Triton-x-100 and paraformaldehyde were from Sigma-Aldrich Chemie GmbH, Munich, Germany. The Transwell filters with a pore size of 0.4 µm and 3 µm were bought from Corning Inc., Corning, USA. RPMI 1650 medium and fetal calf serum Gold (FCS Gold) were from PAA Laboratories GmbH, Cölbe, Germany, Na-pyruvate solution from Cambrex GmbH, Taufkirchen, Germany. Xylol, alcian blue, nuclear fast red and Roti-Histokitt were purchased from Carl Roth GmbH + Co. KG, Karlsruhe, Germany. Leica Histowax paraffin was bought from Leica Microsystems Inc, Bannockburn, USA.

CHARACTERIZATION OF THE POLYSTYRENE MODEL PARTICLES. Size and zeta-potential measurements were performed with a Zetasizer Nano SZ (Malvern Instruments, Herrenberg, Germany). Size was determined with a 173° backscatter angle at 25 °C and an equilibration time of 2 min; the values were calculated as the intensity weighed z-average of three runs with at least 10 subruns each. Zeta-potential was measured with Laser Doppler Electrophoresis in monomodal mode with folded capillary electrophoresis cells at a 17° angle. The average was calculated from three runs (10-100 subruns each).

PERMEATION OF POLYSTYRENE NPs ACROSS CELL-FREE FILTERS OF DIFFERENT PORE SIZES Polystyrene nanoparticles with a diameter of 0.05 µm, 0.1 µm or 0.2 µm, carboxylated or plain, were dispersed in KRB + 1 % bovine serum albumin in a

concentration of 224 µg/ml (corresponding to a concentration of 100 µg/cm^2). Particle size and zeta-potential of the particles are summarized in table 1. The apical compartments of the Corning Transwell filters with a pore diameter of 0.4 µm or 3 µm were filled with 0.5 ml of particle dispersion. The basolateral side was filled with KRB + 1 % BSA and incubated under shaking at 200 rpm for 6 h at 37 °C in an incubator. After 6 h, samples from apical as well as from the basolateral compartments were taken and fluorescence read out (λ_{ex}= 485/20 nm; λ_{em}= 530/30 nm, Multiwell Plate Reader from Tecan Group Ltd., Maennedorf, Switzerland) to quantify the amount of particles in each compartment. Total recovery was determined as the amount of nanoparticles in the apical and basolateral compartment in comparison to the initially applied amount and was found as 100 ± 10 %.

Table 1: Characteristics of the model polystyrene nanoparticles used for the conformation of functionality of the modified Calu-3 Transwell model (particle concentration was 224 µg/ml; n=3; mean ± sd).

	size (Z-average) [nm]		zeta-potential [mV]	
	deionized water	KRB + 1 % BSA	deionized water	KRB + 1 % BSA
p50	76±2	67±1	-42.8±1.5	-6.9±1.7
p100	120±1	138±1	-47.2±0.5	-7.6±0.3
c50	57±1	69±1	-33.2±0.6	-8.8±0.9
c100	99±1	136±1	-37±1.1	-7.5±2.3
c200	207±4	237±1	-33.5±1.6	-8.4±0.7

CALU-3 CELL CULTURE. Calu-3 cells from American Type Culture Collection, Manassas, USA, were grown in RPMI 1650 medium with a supplement of 5 ml of Na-pyruvate and 10 % FCS Gold up to 90 % of confluence and subcultured once a week in a ratio of 1:5 to 1:7. The passages from 28 to 50 were used for experiments. For the preparation of transport assays, 8.93*10^4 cells/cm^2 were seeded in Transwell inserts with a diameter of 1.12 cm^2 and cultured for 7-10 days prior to use. Only cell monolayers with TEER values of > 800 Ωcm^2 were used for experiments.

HISTOLOGICAL EXAMINATION OF CALU-3 CELLS ON FILTERS WITH DIFFERENT PORE SIZES. Cell layers grown on filters with 0.4 µm or 3 µm were cut off from the Transwell inserts including the filter membrane at day 10 or 7 respectively and fixed in 4 % paraformaldehyde in PBS. The filters were embedded into paraffin, cut in 4 µm slices and collected on glass slides. After prewarming them for 15 min at 37 °C, the samples were incubated in xylol for 5 min prior to incubation in a descending isopropanol series for 5 min for each alcohol concentration (100 %, 96 % and 70 % in deionized water). After rinsing in deionized water for 5 min, the samples were dyed with alcian blue (in 3 % acetic acid) for 30 min prior to rinsing with deionized water. Then, the samples were incubated with nuclear fast red and rinsed with deionized water again. After incubation in an ascending isopropanol series (conversely to the descending series) the samples were kept in xylol for 5 min and covered with Roti-Histokitt.

TEER PROFILE OF CALU-3 CELLS. The cells were cultured as described above and seeded into the filter inserts with a density of 6.7*10^4, 8.93*10^4 or 1.12*10^5 cells/cm^2. TEER values were measured with a voltohmmeter equipped with STX-2 chopstick electrodes (Evom from World Precision Instruments, Berlin, Germany) directly after seeding and then before every change of medium, until the TEER values clearly have passed their maximum.

TRANSPORT ASSAY WITH THE MODEL SUBSTANCE SODIUM-FLUORESCEIN. The test substance was dissolved in KRB in a concentration of 30 µM and added to the apical side. Samples were taken from the basolateral compartment directly after application, after 15 min, 30 min, 45 min, 60 min, 90 min and 120 min, the volume was refilled with prewarmed KRB. Na-fluorescein was quantified with a Tecan Multiwell reader (λ_{ex}= 485/20 nm; λ_{em}= 530/30 nm).

Transport assays without cells were performed in the same way, except the sampling intervals were shortened to 2 min, 5 min, 7 min, 10 min and 15 min.

TRANSPORT EXPERIMENTS WITH POLYSTYRENE MODEL PARTICLES. The particles used for permeability experiments of the blank filters were also used for transport experiments with Calu-3 cells. The cells were incubated with 224 µg/ml of particle dispersed in KRB + 1 % BSA for 6 h. The quantification was performed as described above and the amount of particles transported was calculated in relation to the initial amount of particles used.

TRANSPORT EXPERIMENTS WITH METAL OXIDE NANOPARTICLES. Prior to use, the particles were sterilized by γ-irradiation as described in a previous work (Schulze et al., 2008)) to avoid contamination of the cells during the transport assay. Also, the snap-on lid glasses and magnetic stirrers were sterilized as described before (Schulze et al., 2008) and particle dispersions prepared under sterile conditions. Cells were grown on filter inserts with a pore size of 3 µm and cultured for 7-10 days. Only cells that reached TEER values of 800 Ωcm^2 or more were used. This threshold was set so high because the TEER values decreased during the incubation time, also the negative controls dropped. At a value of 800 Ωcm^2 we were sure that the cells maintained a TEER value above the critical threshold of 450 Ωcm^2 (Ehrhardt et al., 2002) for at least the first six hours of incubation. The preparation of the particle dispersion was following the protocol of the project NanoCare we described earlier (Schulze et al., 2008). In a concentration of 224 µg/ml (corresponding to 100 µg/cm^2), the particles were dispersed in RPMI 1650 medium + 10 % FCS Gold. The incubation time was 6 or 24 h at 37 C° under gentle shaking (200 rpm). Before incubation, 0.1 ml from each compartment was taken and diluted in 9.9 ml of the dispersion medium. At the end of the experiment, TEER was checked. The apical as well as the basolateral compartment were extracted and washed 3 times with dispersion medium (apical compartments with 0.5 ml, basolateral compartments with 1.5 ml). The samples of each compartment were pooled in a test tube and filled up to a volume of 10 ml, leading to a dilution of 1:20 for the apical and 1:6.7 for the basolateral compartments. For determination of the amount of nanoparticle in the cell layer and filter membrane, the Transwells were immersed with 4 ml of dispersion medium + 1 % Triton-x-100 and incubated for 0.5 h at 37 °C under gentle shaking. Finally, those 4 ml were withdrawn by suction and pooled with the dispersion medium from two washing steps (2 x 3 ml of dispersion medium + 1 % Triton-x-100, leading to a total volume of 10 ml). A volume of 10 ml was needed due to analytical reasons. All samples were frozen at -80 °C until quantification of the metal with inductively coupled plasma mass spectrometry (ICP-MS) or inductively coupled plasma optical emission spectrometry (ICP-OES).

Table 2: Characteristics of the used metal oxide nanoparticles; *measured in DMEM + 10 % FCS; values adopted from Kroll and colleagues (Kroll et al., 2011)

sample	chemical composition, crystallinity	mean particle size, morphology	BET surface area [m^2/g]	surface chemistry [AT%]	organic modify-cation	pH	zeta-potential [mV]*
ZrO_2	ZrO_2, monoclinic Baddelyite tetragonal	14 nm, irregular but globular	122	O 55 Zr 21 C24 Cl 0.6	organic acid with mass = 180 g/mol	3.7	-8.7±0.8
AlOOH	82.7 % AlOOH; impurities:C, Na, Fe, Si, Li, B	40 nm, irregular but globular	47	O 62 Al 32 C 7	none	4.3	-7.6±0.8
TiO_2 A	O 58 % Ti 41 % Cl< 1 % anatase 95 %, rutile 5 %	17 nm, irregular but globular	117	O 53 Ti 21 C 25 Cl 1	yes	5.4	-6.7±0.7
TiO_2 B	> 99.5 % TiO_2, rutile and anatase, tetragonal	27 nm, irregular but globular	52	O 58 Ti 26 C 14 Cl 1	none	6.1	-9.1±0.3
CeO_2 A	> 99.97 % purity	14 nm, cubic, aggregated	63	O 57 Ce 25 C 18	none	5.9	-9.9±0.5
CeO_2 C	> 99 % CeO_2, Cerianite, cubic	70 nm, irregular but globular	33	O 53 Ce 26 C 20 Cl 0.6	none	5.9	-7.3±1.1

QUANTIFICATION OF METAL OXIDE NANOPARTICLES. Only the metal ion was quantified and afterwards related by means of atomic mass to the nanoparticle oxides. Furthermore, all dilution factors were taken into account. Quantification of ZrO_2 and AlOOH were performed with ICP-OES:

ZrO_2. Standard Zr solutions in 3 % HCl in H_2O (200 ppm, 100 ppm, 20 ppm, 10 ppm, 2 ppm, 1 ppm) were prepared and diluted 1:10 in RPMI medium + 10 % FCS to prepare a calibration line. The accuracy of the calibration line was controlled by comparison to the Zr-specific signals at 343.823 nm and 339.198 nm. Measurements were performed with a Spektro Flame D with a Crossflow vaporizer and a flow of 1.6-1.8 ml/min (high frequency generator 1200 W). At the sample injector equilibrium was established by a higher flow rate for 15 s. Samples were measured and compared to the calibration line to quantify the Zr concentration of the samples. After 15-20 measurements, the optics were repositioned and the calibration line re-measured before further sample investigation. The resulting Zr concentrations were converted to the corresponding ZrO_2 amount.

AlOOH. 200 ppm of AlOOH was solubilized in concentrated H_2SO_4 prior to dilution in 1 % H_2SO_4 to a calibration line (concentrations 50 ppm, 20 ppm, 10 ppm, 2 ppm, 1 ppm). The calibration line was controlled by measurement of an Al standard solution (1 mg/ml) at 394.401 nm and 396.152 nm. Sample measurement was performed analogue to Zr and also converted to the corresponding AlOOH amount.

CeO_2 A and C and TiO_2 A and B were quantified using ICP-MS:

CeO_2 A and C. After disintegration of the particles with nitric acid, the Cerium content of the solution was determined with ICP-MS (Agilent 7500a), with a Meinhardt vaporizer and a 1300 W generator. As an internal standard, ^{45}Sc was used; the limit of detection was 0.1 ppm for the metal ion.

TiO_2 A and B. Thawed and homogenized samples were disintegrated with nitric acid and hydrofluoric acid by means of pressurized vessel digestion in a microwave autoclave (UltraClave III, Milestone, Leutkirch, Germany). Measurement was performed by ICP-MS (ThermoFisher, X-Series-2, Bremen, Germany). The instrument was equipped with a microconcentric nebulizer (AHF, Tübingen, Germany) and run at a generator power of 1300 W. Indium was used as internal standard at a concentration of 1 µg/l. ^{49}Ti was used as the analyte isotope for the evaluation of the results. According to the lowest calibration point the limit of quantification was estimated at 0.5µg/ml.

PHYSICO-CHEMICAL CHARACTERIZATION OF THE METAL OXIDE NANOPARTICLES. For detailed characteristics of the particles, see Table 2. The particles were varying in their bulk material, although we investigated two TiO_2 particles, with or without organic modification. Also, we used two CeO_2 particles, whereas the CeO_2 A particles had a smaller primary particle size, a much bigger surface and were slightly less acidic than CeO_2 C.

RESULTS AND DISCUSSION

Adaptations of the Calu-3 air-blood barrier model to nanoparticles. Normally, filters with a pore size of 0.4 µm are used within the Transwell inserts, but as shown in Figure 2, this filter material even used without a cell layer provided a significant barrier to particles up to 200 nm. Hence, filters with a pore size of 3 µm were tested. Clearly, this change revealed a transport up to total concentration equilibrium after an incubation period of 6 hours, which is a prerequisite for further studies with cell layers.

These results indicated that the use of filter inserts with a pore size of 3 µm is needed to perform particle-related transport assays without taking the likelihood of wrong negative results.

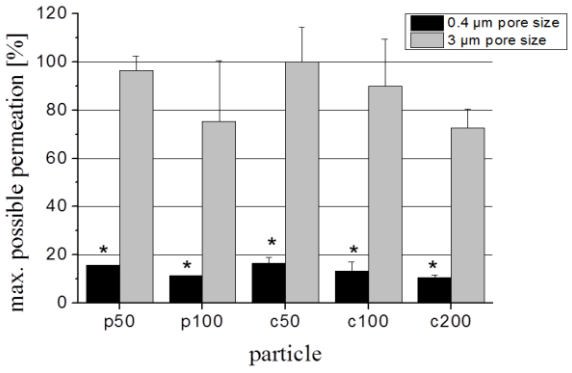

Figure 2: *Permeation of model particles through blank filters with different pore sizes: After 6 h of incubation, up to 100 % of the particles permeated through the filter with the large pores, whereas a pore size of 0.4 µm was a significant barrier for particle permeation (c=carboxylated; p=plain; the number corresponds to the particle diameter; shaking rate 200 rpm; mean + sd; statistics: One way ANOVA, followed by pair wise multiple comparison with Holm-Sidak-method, $p \leq 0.05$; $n = 3$).*

Since the larger pore size is very big relative to the cells used, the relevant cell characteristics had to be investigated. As mentioned in Figure 1, the cells could grow into the pores or even on both sides of the filters, leading to a reinforcement of the barrier and hence falsify permeation rates. Comparison of cross sections of Calu-3 cells on filter inserts with 0.4 µm or 3 µm pore size respectively did not

reveal any visible difference in morphology (Figure 3). Also, the cells did grow only on the surface of the filters. No invasion into the pores or even growth on both sides of the filters occurred.

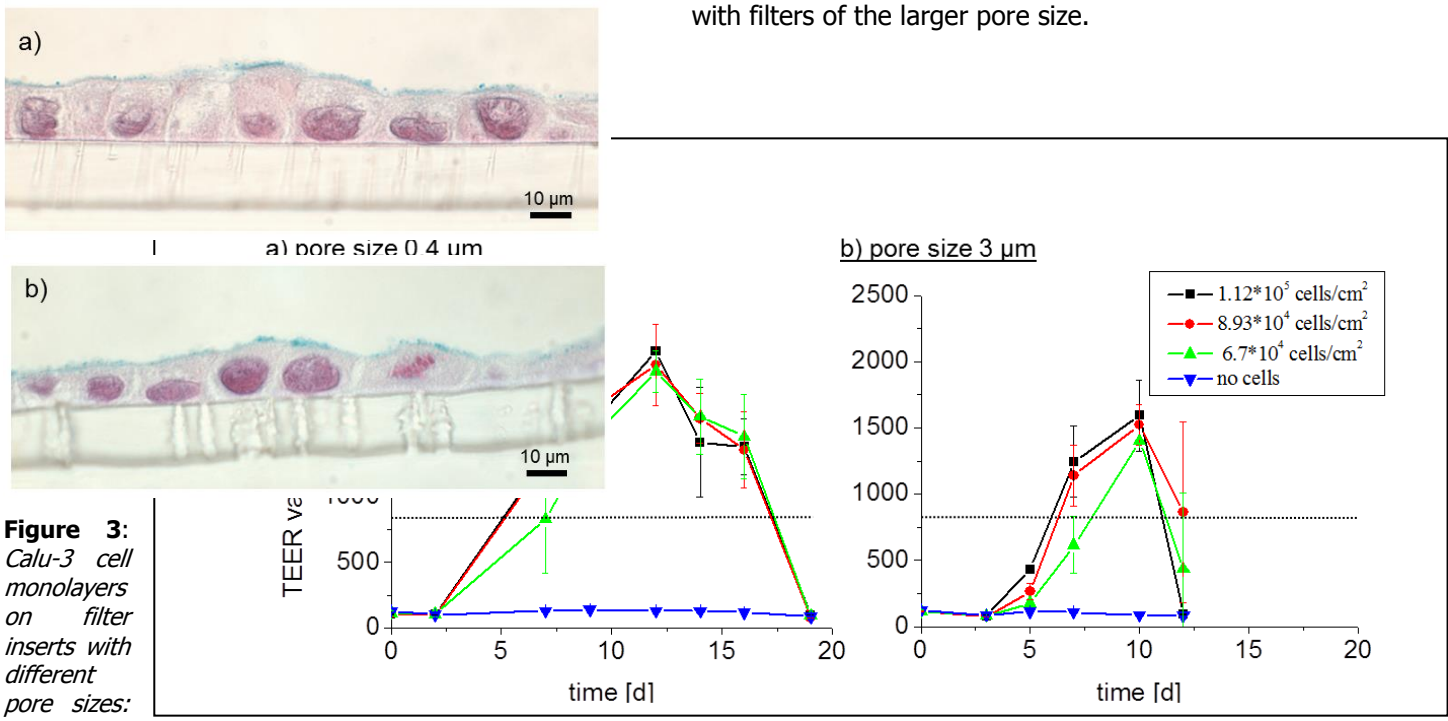

Figure 3: *Calu-3 cell monolayers on filter inserts with different pore sizes: a) pore size of 0.4 µm, Calu-3 cells at day 7; b) pore size of 3 µm, Calu-3 cells at day 10. Clearly, the different size of the pores can be recognized. Both pictures show a confluent cell monolayer without intercellular spaces. Also, a mucus layer of similar height can be detected on both samples. Hence, no differences in morphology can be seen for both monolayers. (seeding density 10^5 cells/cm^2; TEER values > 800 Ωcm^2; magnification 100x).*

Still, similar morphologies alone are no sufficient indicator for analogous barrier properties. Hence, we investigated the integrity of the monolayer by measuring the TEER profile, which is a good method for determining an intact epithelial barrier function (Ehrhardt et al., 2002). As can be seen in Figure 4, Calu-3 cells grown on filter inserts with both pore sizes reached TEER values of more than 800 Ωcm^2, but the maximum for cells grown on the filters with 3 µm pores was lower than for the smaller pore size. Also, the time frame in which the cells maintained these high TEER values was for the larger pore size much shorter (4 days) than for the cells on the smaller pores (up to 10 days). For Calu-3 cells on filters with 0.4 µm pores, a seeding density of $6.7 \cdot 10^4$ cells/cm^2 was sufficient, whereas the optimal seeding density for growth on larger pores should be increased to $8.93 \cdot 10^4$ cells/cm^2, as less cells lead to a slower increase of TEER values and a shortened time period for experiments (Figure 4). In literature, TEER values from 400 to 600 Ωcm^2, but also from 700 up to 2500 Ωcm^2 were reported (Foster, 2000; Furuse, 1994; Loman, 1997). Geys et al. postulated the Calu-3 monolayers to be tight at a TEER of 575 Ωcm^2 for the 0.4 µm pores and at 420 Ωcm^2 for filters with 3 µm pore size (Geys et al., 2006). Although differences in the TEER profile could be detected, an intact barrier function seemed to be given also with filters of the larger pore size.

Figure 4: *TEER profiles of Calu-3 cells grown on filter inserts with different pore sizes: Both pore sizes lead to TEER values of more than 1000 Ωcm2, although the time lines are varying. For Calu-3 cells on filters with a pore size of 3 µm the maximum is lower and is reached earlier than on filters with the smaller pore size. Also, the time frame for experiments is with 4 days for the larger pores size shorter than 10 days, respectively (mean ± sd, n=9).*

Although the integrity of the monolayer could be proven by TEER, we wanted to confirm these results by testing the transport of the low permeability marker Na-fluorescein. The results are

Table 3: P_{app} values for Na-fluorescein as low permeability marker, tested with and without cell monolayers, to confirm similar transport patterns for Calu-3 cells on both filter inserts (TEER for experiments containing Calu-3 cells > 800 Ωcm^2 before and after transport assays; mean ± sd, n=3).

pore size	filter only [cm/s]	cell monolayer [cm/s]
0.4 µm	$3.83 \pm 0.09 \cdot 10^{-5}$	$1.61 \pm 0.05 \cdot 10^{-7}$
3 µm	$20.6 \pm 0.5 \cdot 10^{-5}$	$9.37 \pm 0.38 \cdot 10^{-7}$
ratio 3 µm/0.4 µm	5.4	5.8

summarized in table 3: The P_{app} value without cells varied considerably from that of filters with cells, i.e. the cell layer is a functioning barrier for the low permeability marker. However, the P_{app} value was about five times higher for the larger pore size with and also without cells. This can be explained with the different filter properties: The total "pore area" of both filters was calculated to be $5 \cdot 10^{-3}$ cm^2 (0.4 µm pore size) or 0.14 cm^2 (3 µm pore size), respectively. This is resulting in a much higher relation of this "pore area" compared to the total filter area, although both filters have equal dimensions (see Figure 1). A larger pore area results in more direct contact between the apical and basolateral compartment. Permeation experiments with Na-fluorescein without cells clearly confirm the higher permeation to be due to the larger diffusion area in favour of the filters with 3 µm pores, as the ratios between the filters of the different pore sizes were very similar (see Table 3). These results confirm that the integrity of the monolayer is not compromised when grown on filters with a pore size of 3 µm.

Transport experiments with polystyrene model particles. As proof of the functionality of the adapted barrier model, transport experiments with polystyrene model particles with a size range from 50 to 200 nm were performed. Clearly, a particle transport of up to 4 % after 24 h of incubation could be seen (Figure 5), which is corresponding well to the transport rates found in literature for Calu-3 cells (Geys et al., 2006). Smaller particles are transported in higher amounts than the larger 200 nm particles, but only the plain 50 nm particle showed a significantly higher transport rate compared to the larger particles. Furthermore, no statistically relevant difference between the transport of plain and carboxylated NPs could be detected. To rule out transport of the fluorescent dye only after cleavage from the particle, the presence of particles in basolateral samples was tested via Dynamic Light Scattering. In all samples, particles could be detected of the same size as applied in the apical compartment.

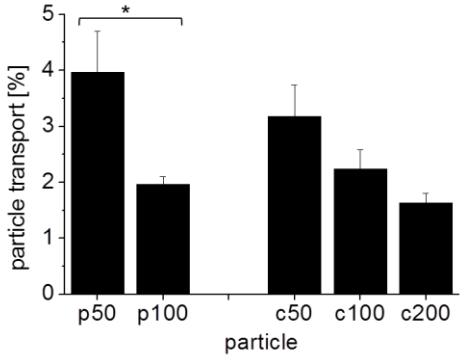

Figure 5: *Transport of model polystyrene particles over Calu-3-cell monolayers grown on supports with 3 µm pore size from apical to basolateral side after an incubation time of 24 h. The TEER for the Calu-3 cells exceeded 800 Ωcm2 before transport assays. Significant differences are marked with a (*) (p=plain particle without surface modifications, c=carboxylated surface; numbers represent the diameter of the particle; mean + sd; statistics: One way ANOVA, followed by pair wise multiple comparison with Holm-Sidak-method, $p \leq 0.05$; n=3).*

Table 4: Summary of transport assays performed with metal oxide nanoparticles after an incubation time of 24 h; Except for both CeO_2 particles, no transport could be detected (n=3; mean ± sd).

nanoparticle	permeation through naked filter [%]	transport through cells after 24 h [%]	cellular uptake & filter washout after 24 h [%]
ZrO_2	54.6 ± 5.8	0	0
AlOOH	62.2 ± 25.5	0	0
TiO_2 A	27 ± 4.9	0	0
TiO_2 B	46.4 ± 5.4	0	0
CeO_2 A	31.9 ± 5.6	3.5 ± 1.3	3.5 ± 1.3
CeO_2 C	75.9 ± 50.2	3.2 ± 0.1	5.5 ± 2.1

Smaller particles seem to be transported in higher amounts than the larger 200 nm particles, but only the plain 50 nm particle showed a significantly higher transport rate compared to the larger particles. A generally increased transport for the plain particles cannot be confirmed. To rule out transport of the fluorescent dye only after cleavage from the particle, the presence of particles in basolateral samples was tested via Dynamic Light Scattering. In all samples, particles could be detected of the same size as applied in the apical compartment.

Transport of metal oxide nanoparticles. The transport assays with metal oxide nanoparticles were performed with a particle concentration of

100 µg/cm^2 (=224 µg/ml) for 6 and 24 h of incubation under sterile conditions. The transport results are summarized in Table 4: All of the particles tested permeated through the naked filter, i.e. the filter pores were no explicit barrier for particle permeation. For ZrO_2, AlOOH and both TiO_2 particles neither a transport nor particle uptake into the cell or adhesion onto the cell surface could be detected. This is in good agreement with *in vivo* short and long-term inhalation studies performed with the very same TiO_2 and AlOOH particles, as no translocation into liver, kidney, spleen or basal brain with olfactory bulb could be detected (Kuhlbusch, 2009; Pauluhn, 2009). In those inhalation studies, also CeO_2 C was tested negative for translocation into the mentioned organs. This is in contrast to our findings, as we could prove a particle transport similar to that of the carboxylated 100 nm model particle (see Figure 5). Also, cerium could be detected in the cell lysates and filter washout samples, indicating a transcellular transport of the CeO_2 particles. The particle concentrations for CeO_2 C in the in vivo study was with a maximum concentration of 10 mg/m^3 (= 0.01 µg/ml) much lower than the concentration tested here (100 µg/cm^2= 224 µg/ml). Therefore, an overload effect of the cells may be a plausible explanation for the transport detected. However, working with lower concentrations in the donor compartments was not possible, as otherwise we dropped below the detection limits of ICP-MS.

The TEER value is simple, but meaningful indicator of an intact epithelial cell monolayer with proper barrier functions (Ehrhardt et al., 2002). Hence, when the monolayer is affected, the TEER is decreasing. Controlling of the TEER before and after the incubation with ZrO_2 particles revealed a significant decrease of TEER after 24 h compared to the negative control (see Table 5). Although the barrier seemed to be disrupted, no ZrO_2 translocation could be detected. In all experiments, also the negative controls, TEER (treated with dispersion medium instead of particle dispersion) decreased after 24 h. The same ZrO_2 particles (concentrations of 0.1 -10 µg/cm^2) tested on MDCK II and NRK52E cells had no effect on TEER (Kuhlbusch, 2009). Hence, the TEER decrease for ZrO_2 is more likely to be due to the experimental procedure or also an overload effect.

As we have proven for polystyrene model particles, some nanomaterials can be transported across the epithelial air-blood barrier model. We used the Calu-3 monoculture model, because there is a lot of transport data available in literature, especially for soluble substances in pharmaceutical research. Also, it is simple and easy to use, which makes it a good entry model. However, an expansion of the epithelial model to a triple cell culture, containing macrophages on the apical and dendritic cells on the basal side, reveals more possibilities of overcoming the epithelial barrier. Blank et al. could show that polystyrene particles with a size of 1 µm were rarely taken up by the epithelial cells, but by the macrophages and the dendritic cells, either by extensions or total migration of the dendritic cells through the epithelium. Also, particle transport between dendritic cells and between macrophages and dendritic cells could be shown (Blank et al., 2007). This particle transport is not disrupting the integrity of the epithelial layer (Blank et al., 2008). Those transport routes might be relevant for the tested particles, too, i.e. a negative result with our model does not guarantee no transport at all.

To test the transport of nanoparticles with the air-blood barrier model Calu-3, the model had to be adapted by adjusting the pore size of the filter inserts the cells are grown on. The cells did not reveal morphological differences grown on filters with different pore sizes. Seeding density had to be adapted, also, the time frame for experiments changed. The transport pattern of the cells was not influenced, as we proved with transport experiments with Na-fluorescein. Functionality of

Table 5: TEER values of the cells after 6 or 24 h of incubation with (=samples) or without nanoparticles (=negative control). The data are relative to the TEER measurements taken immediately before incubation (mean ± sd). The only particle revealing a significant decrease in barrier function compared to the negative control is ZrO_2 after an incubation for 24 h (n = 3; p≤0.05).

	TEER after 6 h incubation [%]		**TEER after 24 h incubation [%]**	
	sample	negative control	sample	negative control
ZrO_2	79.7 ± 9.7	86.6 ± 2	47.4 ± 6.8	69.8 ± 3.5
AlOOH	58.5 ± 10.6	47.7 ±3.4	29.6 ± 1.3	49.8 ± 16.3
TiO_2 A	82.9 ± 5.1	68.1 ± 6.4	29.6 ± 3.7	23.8 ± 3.7
TiO_2 B	85.1 ± 2.3	83.6 ± 5	21.1 ± 0.2	21.4 ± 1.3
CeO_2 A	104.3 ± 26.2	74 ± 17.8	39 ± 8.9	34.4 ± 9.6
CeO_2 C	54.9 ± 17.3	46.3 ± 6.8	43.3 ± 5.9	37.4 ± 6.2

the model was proven with polystyrene model particles prior to experiments with metal oxide nanoparticles. Although the TEER values decreased in all experiments, no translocation was detected for ZrO_2, TiO_2 A and B and for AlOOH. Only CeO_2 A and C revealed a transport. As metal oxide nanoparticles are not easily detected and quantified, determination of transport rates is a challenging task, whereas the optimal experimental setup is still to be improved.

Acknowledgements

Leon Muijs is thanked for the preparation of the Calu-3 cross sections and histological staining. Also, ItN Nanovation AG is thanked for the characterization of the TiO_2 A particles. The Federal Ministry of Education and Research BMBF (Project "NanoCare", Förderkennzeichen 03X0021C) is thanked for financial funding.

References

AshaRani, P.V., Low Kah Mun, G., Hande, M.P., and Valiyaveettil, S. (2009). Cytotoxicity and genotoxicity of silver nanoparticles in human cells. ACS nano *3*, 279-290.

Blank, F., Rothen-Rutishauser, B., and Gehr, P. (2007). Dendritic cells and macrophages form a transepithelial network against foreign particulate antigens. Am J Respir Cell Mol Biol *36*, 669-677.

Blank, F., Wehrli, M., Baum, O., Gehr, P., and Rothen-Rutishauser, B. (2008). The epithelial integrity is preserved during particle exchange across the epithelium by macrophages and dendritic cells. Eur Respir Rev *17*, 78-80.

Carlson, C., Hussain, S.M., Schrand, A.M., Braydich-Stolle, L.K., Hess, K.L., Jones, R.L., and Schlager, J.J. (2008). Unique cellular interaction of silver nanoparticles: size-dependent generation of reactive oxygen species. J Phys Chem *112*, 13608-13619.

Choi, J.Y., Lee, S.H., Na, H.B., An, K., Hyeon, T., and Seo, T.S. (2009). In vitro cytotoxicity screening of water-dispersible metal oxide nanoparticles in human cell lines. J Inorg Biochem 103, 463-71.

Ehrhardt, C., Fiegel, J., Fuchs, S., Abu-Dahab, R., Schaefer, U.F., Hanes, J., and Lehr, C.M. (2002). Drug absorption by the respiratory mucosa: cell culture models and particulate drug carriers. *J Aerosol Med 15*, 131-139.

Florea, B.I., Cassara, M.L., Junginger, H.E., and Borchard, G. (2003). Drug transport and metabolism characteristics of the human airway epithelial cell line Calu-3. J Control Release *87*, 131-138.

Forbes, B., and Ehrhardt, C. (2005). Human respiratory epithelial cell culture for drug delivery applications. Eur J Pharm Biopharm *60*, 193-205.

Foster, K.A., Avery, M.L., Yazdanian, M., Audus, K.L. (2000). Characterization of the Calu-3 cell line as a tool to screen pulmonary drug delivery. Int. J. Pharm. *208*, 1-11.

Furuse, M., Itoh, M., Hirase, T., Nagafuchi, A., Yonemura, S., Tsukita, S. (1994). Direct association of occludin with ZO-1 and its possible involvement in the localization of occludin at tight junctions. J. Cell Biol. *127*, 1617-1626.

Geys, J., Coenegrachts, L., Vercammen, J., Engelborghs, Y., Nemmar, A., Nemery, B., and Hoet, P.H. (2006). In vitro study of the pulmonary translocation of nanoparticles: a preliminary study. Toxicol Lett *160*, 218-226.

Hillaireau, H., and Couvreur, P. (2009). Nanocarriers' entry into the cell: relevance to drug delivery. Cell Mol Life Sci *66*, 2873-2896.

Kreyling, W.G., Semmler-Behnke, M., Seitz, J., Scymczak, W., Wenk, A., Mayer, P., Takenaka, S., and Oberdorster, G. (2009). Size dependence of the translocation of inhaled iridium and carbon nanoparticle aggregates from the lung of rats to the blood and secondary target organs. Inhal Toxicol *21 Suppl 1*, 55-60.

Kroll, A., Dierker, C., Rommel, C., Hahn, D., Wohlleben, W., Schulze-Isfort, C., Gobbert, C., Voetz, M., Hardinghaus, F., and Schnekenburger, J. (2011). Cytotoxicity screening of 23 engineered nanomaterials using a test matrix of ten cell lines and three different assays. Part Fibre Toxicol *8*, 9.

Kuhlbusch, T.A.J., Krug, H.F., Nau, K., ed. (2009). NanoCare Health related Aspects of Nanomaterials Final Scientific Report, 1 edn (Frankfurt a.M., Dechema e.V.).

Lehr, C.M., Bur, M., and Schaefer, U.F. (2006). Cell culture models of the air-blood barrier for the

evaluation of aerosol medicines. Altex *23 Suppl*, 259-264.

Loman, S., Radl, J., Jansen, H.M., Out, T.A., Lutter, R. (1997). Vectorial transcytosis of dimeric IgA by the Calu-3 human lung epithelial cell line: upregulation by IFN-gamma Am. J. Physiol. *272*, L951-L958.

Mathia, N.R., Yamashita, F., and Lee, V.H.L. (1996). Respiratory epithelial cell culture models for evaluation of ion and drug transport. Adv Drug Deliv Rev *22*, 215-249.

Pauluhn, J. (2009). Pulmonary toxicity and fate of agglomerated 10 and 40 nm aluminum oxyhydroxides following 4-week inhalation exposure of rats: toxic effects are determined by agglomerated, not primary particle size. Toxicol Sci *109*, 152-167.

Rothen-Rutishauser, B.M., Kiama, S.C., and Gehr, P. (2005). A three-dimensional cellular model of the human respiratory tract to study the interaction with particles. Am J Respir Cell Mol Biol *32*, 281-289.

Sakagami, M. (2006). In vivo, in vitro and ex vivo models to assess pulmonary absorption and disposition of inhaled therapeutics for systemic delivery. Adv Drug Deliv Rev *58*, 1030-1060.

Schulze, C., Kroll, A., Lehr, C.M., Schaefer, U.F., Becker, K., Schnekenburger, J., Schulze Isfort, C., Landsiedel, R., and Wohlleben, W. (2008). Not ready to use - Overcoming pitfalls when dispersing nanoparticles in physiological media. Nanotoxicology *2*, 51-61.

Sporty, J.L., Horalkova, L., and Ehrhardt, C. (2008). In vitro cell culture models for the assessment of pulmonary drug disposition. Expert Opin Drug Metab Toxicol *4*, 333-345.

Wahl, B., Daum, N., Ohrem, H.L., and Lehr, C.M. (2008). Novel luminescence assay offers new possibilities for the risk assessment of silica nanoparticles. Nanotoxicology *2*, 243-251.